Mobility of discrete multibreathers in the exciton dynamics of the Davydov model with saturable nonlinearities

J. D. Tchinang Tchameu,* A. B. Togueu Motcheyo,† and C. Tchawoua‡

Laboratory of Mechanics, Department of Physics, Faculty of Science, University de Yaounde I, P.O. Box 812, Yaounde, Cameroon

(Received 27 May 2014; published 21 October 2014)

We show that the state of amide-I excitations in proteins is modeled by the discrete nonlinear Schrödinger equation with saturable nonlinearities. This is done by extending the Davydov model to take into account the competition between local compression and local dilatation of the lattice, thus leading to the interplay between self-focusing and defocusing saturable nonlinearities. Site-centered (sc) mode and/or bond-centered mode like discrete multihump soliton (DMHS) solutions are found numerically and their stability is analyzed. As a result, we obtained the existence and stability diagrams for all observed types of sc DMHS solutions. We also note that the stability of sc DMHS solutions depends not only on the value of the interpeak separation but also on the number of peaks, while their counterpart having at least one intersite soliton is instable. A study of mobility is achieved and it appears that, depending on the higher-order saturable nonlinearity, DMHS-like mechanism for vibrational energy transport along the protein chain is possible.

DOI: 10.1103/PhysRevE.90.043203 PACS number(s): 05.45.Yv, 87.14.E−, 63.20.Pw, 71.35.−y

I. INTRODUCTION

During many biological processes, such as muscle contraction, DNA reduplication, neuroelectric pulse transfer on the neurolemma, and work of calcium or sodium pump, the bioenergy needed is provided by the hydrolysis of adenosine triphosphate (ATP). This energy has important significance and the comprehension of their storage and transport has been a challenge to scientists. In 1973, Davydov [1] suggested a mechanism based on soliton to elucidate the problem. Since the previous mentioned work, the possible existence of solitons in biomolecular systems has been widely studied (see Ref. [2], and references therein). Following Davydov's idea, energy released during ATP hydrolysis is stored in the form of a vibrational energy of the C=O stretching (amide-I) oscillators. This energy is transported from one peptide group to the next because of the dipole-dipole coupling between the adjacent groups. Experimentally, the model of Scott and Davydov was tested through the crystalline polymer acetalinide ($(CH_3CONHC_6H_5)_X$), or ACN, which is an organic solid close to a biological molecule [3].

At low temperature it has been shown that Davydov's theory for the α-helix gives rise to discrete nonlinear Schrödinger (DNLS) equation [4], which is one of the basic lattice models appearing in various contexts of physics and biology. During the past decade, DNLS equations as well as one of their solutions called discrete breather (alias intrinsic localized modes) have been intensively studied [5,6]. Discrete breather has a bell-shaped form while ones possessing an arbitrary number of extrema is called multibreather. Proof of the existence of the latter is given in Ref. [7], and since this work a great deal of effort has been invested to show their existence in Salerno equation [8], DNLS equation with cubic nonlinearity [9], and Klein-Gordon chain [10]. More recently, multibreathers have been predicted theoretically in realistic systems [11] and observed experimentally [12]. In spite the fact that multihump soliton have been observed in saturable dispersive nonlinear medium [13], their study is not yet done in purely discrete saturable nonlinear equation. The first purpose of this work is to explore the possible existence of multibreathers in DNLS equation with saturable nonlinearities.

At the beginning of the year 2000, the stability of multibreathers was an open problem (see Ref. [14]). Up to now much effort has gone into their stabilization [10–12,15], and it's well clear that stable multibreathers can be found. Could we obtain stable multibreathers in the exciton dynamics modeled by DNLS equation with competitive nonlinearities? The answer to this question is the second purpose of this work.

It has been observed for several years that discrete breathers could be mobile in some models [16–24]. To the best our knowledge, a study related to the mobility of multibreathers is not yet done. As the last aims of this work, we look for the possible mobile multibreathers in the system.

The rest of the paper is organized in the following manner. In Sec. II, the DNLS equation with saturable nonlinearities, which describes the state of amide-I excitations in proteins is derived. In Sec. III, we look for the discrete multihump solitons solutions of the previous-mentioned equation. Section IV is devoted to the mapping and linear stability analysis of these solutions. This section ends with the existence and stability diagrams for all observed types of discrete multihump soliton solutions. In Sec. V, we investigate the potential mobility of these solutions. Finally, the conclusion summarizing the different results of this work is given in the Sec. VI.

II. THE DAVYDOV MODEL AND DISCRETE NONLINEAR SCHRÖDINGER EQUATION WITH SATURABLE NONLINEARITIES

Let us consider the Davydov model with exciton-phonon coupling in hydrogen-bonded molecular chains. This infinite discrete chain consists of peptide groups (H-N-C=O) with a mass M, regularly spaced by a distance R, and

*jtchinang@gmail.com
†abtogueu@yahoo.fr
‡Corresponding author: ctchawa@yahoo.fr

weakly bound according to the following sequence: $\cdots$H-N-C=O$\cdots$H-N-C=O$\cdots$H-N-C=O$\cdots$H-N-C=O$\cdots$. The dotted lines represent the hydrogen bonding. In addition, the interaction is assumed to work only between nearest-neighbor molecules.

The Hamiltonian associated with the network so described is expressed as

$$H = T + U + \sum_n [(\varepsilon - D_n)B_n^+ B_n - J(B_{n+1}^+ B_n + B_{n+1} B_n^+)], \tag{1}$$

where T is kinetic energy and U is the potential energy. The first part of the third term, $\varepsilon B_n^+ B_n$, defines the amide-I excitation energy, and the fourth term stands for the resonance dipole interaction between nearest neighbors. This interaction is characterized by the dipole-dipole interaction energy J. Notice that B_n^+ (B_n) is the creation (annihilation) operator of the amide-I excitation in the nth group. In the second part of the third term, the function $-D_n$ represents the deformation excitation energy of the nth peptide group with its nearest neighbors and can be written as [25]

$$D_n = \mathcal{D}_n(|x_{n+1} - x_n|) + \mathcal{D}_n(|x_n - x_{n-1}|). \tag{2}$$

Then, $-D_n B_n^+ B_n$ describes the interaction between the intramolecular excitation and the lattice displacements. Assuming that the coupling is strong, because it has been shown [26] that autolocalized excitation solitons appear in the system due to the nonlinear and strong exciton-phonon interaction, Eq. (2) can be written in the form

$$D_n \approx \left(1 + \frac{\beta}{R}\rho_n - \frac{\gamma}{2R^2}\rho_n^2\right) D, \tag{3}$$

where

$$\rho_n = R - |x_n - x_{n-1}| \tag{4}$$

denotes the relative distances between two neighboring groups from equilibrium and x_n, the small displacement of the nth peptide groups. Add that β and γ are adjustable positive parameters of the deformation excitation energy while $D = 2\mathcal{D}(R)$. Comparing Eq. (3) to one used in Ref. [27], the choice of the negative sign of the last term here is to take into account the competition between local compression and local dilation of lattice.

The use of Born-Oppenheimer approximation leads us to consider the lattice displacements as classical variables. This is justified by the fact that the effective mass M of the peptide group is large, thus leading acoustic vibrations to be slow compared to the excitonic modes. In order to establish the equations of motion, we define the soliton wave function as

$$|\psi\rangle = \sum_n a_n(t) B_n^+ |0\rangle, \tag{5}$$

where $|0\rangle$ is the vacuum state and a_n is the complex probability amplitude of the exciton wave, which satisfies the normalization condition

$$\langle\psi|\psi\rangle = \sum_n |a_n(t)|^2 = 1. \tag{6}$$

Using time-dependent Schrödinger equation and Heisenberg equation we obtain the system of coupled equations

$$i\hbar \frac{\partial a_n}{\partial t} = \left[\varepsilon + T + U - \left(1 + \frac{\beta}{R}\rho_n - \frac{\gamma}{2R^2}\rho_n^2\right) D\right] a_n - J(a_{n+1} + a_{n-1}), \tag{7}$$

$$M\frac{\partial^2 \rho_n}{\partial t^2} = -\omega(2\rho_n - \rho_{n+1} - \rho_{n-1}) + \frac{\beta D}{R}(2|a_n|^2 - |a_{n+1}|^2 - |a_{n-1}|^2) - \frac{\gamma D}{R^2}(2\rho_n|a_n|^2 - \rho_{n+1}|a_{n+1}|^2 - \rho_{n-1}|a_{n-1}|^2), \tag{8}$$

where ω is the spring constant. $T = \frac{M}{2}\sum_n (\frac{\partial x_n}{\partial t})^2$ and $U = \frac{\omega}{2}\sum_n \rho_n^2$. The great value of M leads to the adiabatic approximation [4]

$$\frac{\partial^2 \rho_n}{\partial t^2} \approx 0. \tag{9}$$

Neglecting the inertia term, we solve Eq. (8) and obtain the following relation:

$$\rho_n = \frac{\frac{\beta D}{R\omega}|a_n|^2}{1 + \frac{\gamma D}{R^2\omega}|a_n|^2}. \tag{10}$$

Then, the substitution of Eq. (10) in Eq. (7) yields

$$i\hbar\frac{\partial a_n}{\partial t} = [\varepsilon + T + U - D]a_n - \nu_1 J \frac{|a_n|^2 a_n}{1 + \nu_3|a_n|^2} + \nu_2 J \frac{|a_n|^4 a_n}{(1 + \nu_3|a_n|^2)^2} - J(a_{n+1} + a_{n-1}), \tag{11}$$

where $\nu_1 = \frac{\beta^2 D^2}{R^2\omega J}$, $\nu_2 = \frac{\gamma\beta^2 D^3}{2R^4\omega^2 J}$, and $\nu_3 = \frac{\gamma D}{R^2\omega}$.

Equation (11) is reduced in the form

$$i\frac{\partial \phi_n}{\partial \tau} = -\Delta_2\phi_n + \eta_1\frac{\phi_n}{1 + |\phi_n|^2} + \eta_2\frac{|\phi_n|^2\phi_n}{(1 + |\phi_n|^2)^2}, \tag{12}$$

if we set

$$\phi_n = \sqrt{\nu_3} a_n \exp i\tau\left[\frac{\varepsilon + T + U - D - 2J - \eta_1 J}{J}\right], \quad \eta_1 = \nu_1/2\nu_3, \quad \text{with} \quad \nu_3 \neq 0,\ \eta_2 = -\eta_1, \tag{13}$$

and use the dimensionless time $\tau = Jt/\hbar$. In Eq. (12), η_1 and η_2 are the strength of the nonlinearities and $\Delta_2\phi_n = (\phi_{n+1} + \phi_{n-1} - 2\phi_n)$.

It is well known that under adiabatic approximation, Davydov shows that the dynamics of the coupled exciton-phonon system is reduced to the DNLS equation [4]. Here, since $\eta_1 > 0$ and $\eta_2 < 0$, Eq. (12) is named the DNLS equation with competitive saturable nonlinearities. This equation has two conserved quantities: the Hamiltonian,

$$E = \sum_n \left[|\phi_{n+1} - \phi_n|^2 + (\eta_1 + \eta_2) \times \log(1 + |\phi_n|^2) + \frac{\eta_2}{1 + |\phi_n|^2} \right], \tag{14}$$

and the number of quanta (l^2-norm),

$$P = \sum_n |\phi_n|^2. \tag{15}$$

We also note that, due to the last term in the right-hand side, Eq. (12) is different from the well-known DNLS equation with photorefractive nonlinearity, widely used in optics. In the other words, the coefficient η_2 guarantees the presence of higher-order saturable nonlinearity. In order to give a physical meaning to η_2, let us set $\eta_1 = -\eta_2 = \eta$ and we consider $\chi_1 = (\beta D/R) > 0$ and $\chi_2 = -(\gamma D/2R) < 0$, the phonon-exciton coupling parameters. χ_1 and χ_2, respectively, represent the parameters of nonlinear coupling. Thus, if $\gamma = 0\,(\chi_2 = 0)$, we have through Eq. (11) $\nu_2 = \nu_3 = 0$, and we get the classical Davydov-Scott model, which leads to the well-known DNLS equation with cubic nonlinearity. Therefore, χ_2 contributes to the strong phonon-exciton coupling, thereby promoting the formation of soliton. Similar considerations have been used by Velarde and coworkers [28], when looking for long-living intrinsic localized solectron, they have considered an extended polaron Hamiltonian in which the electron-hopping term is affected by anharmonicity. In the following, we parametrize our problem by η, which is also expressed as $\eta = (\chi_1 R/4J)\widetilde{\eta}$, with $\widetilde{\eta} = -(\chi_1/\chi_2)$. For α-helical proteins, the use of the following physical parameters [29,30] $J = 9.67 \times 10^{-4}$ eV, $\chi_1 = 8 \times 10^{-2}$ eV/Å, $\omega = 0.8125$ eV/Å^2, $R = 4.5$ Å, leads to $\eta \approx 93\widetilde{\eta}$.

Based on the meaning of the sign of χ [31], it appears that negative coefficient means that the molecular chain is locally dilated (dilatational soliton) and a positive value represents the local compression (compressional soliton) of molecular chain due to amide-I vibrations. It follows that our model exhibits a competition of self-focusing (dilatation) and defocusing (compression) saturable nonlinearities. This is a good compromise given the fact that in the literature, the coupling parameter is taken positive or negative [32].

It is also important to recall that an equation similar to Eq. (11) has been obtained by Aguero [27] in a continuous medium. However, to look for the soliton structures, he has simplified the equation to cubic-qintic nonlinear Schrödinger equation in order to solve it. So, in the next section, we will determine discrete multisoliton (discrete multibreather) solutions of Eq. (12).

III. DISCRETE STATIONARY MULTIHUMP SOLITON SOLUTIONS

In order to solve Eq. (12) governing the evolution of the complex probability amplitude ϕ_n, we seek the stationary solutions of the form $\phi_n = u_n \exp(-i\Omega\tau)$, Ω being a frequency. Under this condition, we obtain a set of coupled algebraic equations for the real function u_n:

$$\Omega u_n + (u_{n+1} + u_{n-1} - 2u_n) - \eta \frac{u_n}{1 + u_n^2} + \eta \frac{u_n^3}{\left(1 + u_n^2\right)^2} = 0. \tag{16}$$

It should be added to the above relations, the normalization condition given by Eq. (6), and rewritten as

$$\sum_n u_n^2 \simeq \frac{0.043}{\widetilde{\eta}}. \tag{17}$$

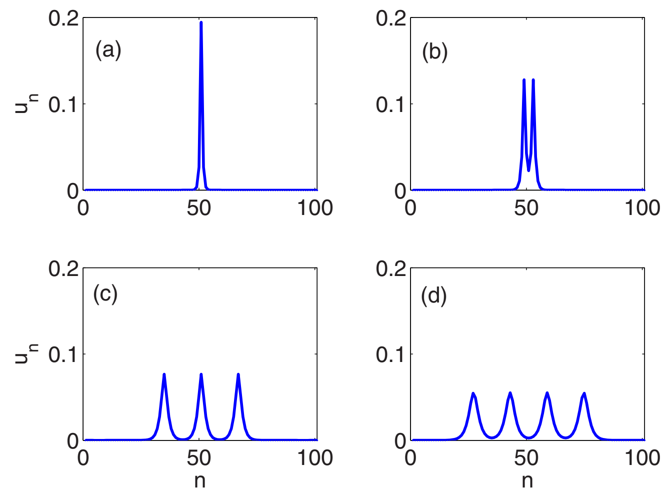

FIG. 1. (Color online) Examples of profiles of single-hump [(a) $(\widetilde{\eta};\Omega) \approx$ (1.1;96.706)], two-hump [(b) $(\widetilde{\eta};\Omega) \approx$ (1.1;100.4)], three-hump [(c) $(\widetilde{\eta};\Omega) \approx$ (1.1;101.75)], and four-hump [(d) $(\widetilde{\eta};\Omega) \approx$ (1.1;102)] solitons.

It is well known that two-component systems with saturable nonlinearity can sustain both single-hump and multihump solitons (optical solitons) [33]. The idea is to investigate the presence of such solutions in our model despite being a one-component system. This is done numerically, by means of iterative multidimensional Newton-Raphson method with periodic boundary conditions and initial guess produced by the high-confinement approximation [34]. These solutions are illustrated in Fig. 1, where we give the profiles of single-hump, two-hump, three-hump, and four-hump solitons for $(\widetilde{\eta};\Omega) \approx (1.1;96.706)$, $(\widetilde{\eta};\Omega) \approx (1.1;100.4)$, $(\widetilde{\eta};\Omega) \approx (1.1;101.75)$, and $(\widetilde{\eta};\Omega) \approx (1.1;102)$, respectively. These discrete stationary multihump solitons are all constituted of solitons belonging to site-centered (sc) mode. Note that multihump solitons composed of solitons belonging to bond-centered (bc) mode and those belonging to bc and sc mode were also found. Figure 2 shows this case with the profile of two-hump and three-hump solitons for bc-sc mode, bc-bc mode, and sc-bc-sc mode. We are now interested in multihump soliton solutions constituted solely of sc modes. Let ℓ_δ represents the interpeak separation, i.e., the distance between two neighbor peaks, where the subscript δ is the number of peak of the solution. In the case of two-hump solitons, we obtain $\ell_2 = 4$ while for three- and four-hump solitons, $\ell_3 = \ell_4 = 4\ell_2 = 16$ (see Fig. 1). This means that the localization of solution decreases when δ increases. Moreover,

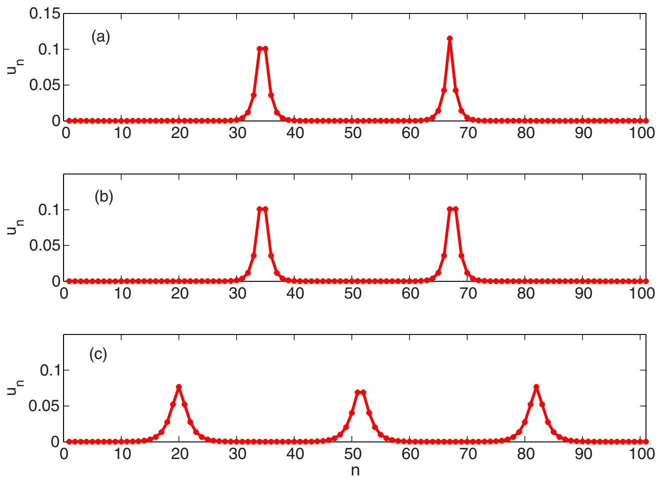

FIG. 2. (Color online) Examples of profiles of two-hump [(a) $(\widetilde{\eta};\Omega)\approx$ (1.1;100.9)], two-hump [(b) $(\widetilde{\eta};\Omega)\approx$ (1.1;100.9)], and three-hump [(c) $(\widetilde{\eta};\Omega)\approx$ (1.1;101.75)] solitons for bc-sc mode, bc-bc mode, and sc-bc-sc mode, respectively.

by noting ζ_δ as being the maximum amplitude of the δ-soliton, we have $\zeta_1 \simeq 0.19$, $\zeta_2 \simeq 0.13$, $\zeta_3 \simeq 0.077$, and $\zeta_4 \simeq 0.055$. So we also see a gradual decrease of ζ_δ as the number of peaks δ increases. It appears from these results that the system cannot admit an unlimited number of peaked localized states. Recall that the normalization condition for envelope u_n ($\sum_n u_n^2 \simeq \frac{0.043}{\widetilde{\eta}}$) is satisfied for all these solutions. We can conclude that the localization of vibrational energy in protein can be in the form of single discrete solitons or a discrete multisoliton. A similar result was obtained in the past in the context of two-component solitary waves [35].

It is important to mention that $\widetilde{\eta}$ not only reflects the saturation coefficient but also the ratio between the expansion and compression terms of the molecular chain. We also want to add the following biological meaning of the phenomenon of saturation in order to show how our model is more realistic. The ATP conserves energy via glycolysis, glycogenolysis, and the citric acid cycle. If the cells have sufficient supplies of ATP, then these pathways and cycles are inhibited. Under these conditions of excess ATP, the liver will attempt to convert a variety of excess glucose molecules into glycogen [36]. Thus, when ATP is too large, there is a saturation through these inhibitions. Otherwise, when the probability amplitude $|\phi_n|$ is low, the saturable nonlinearities can be reduced to a cubic nonlinearity via a Taylor expansion. Thus, the feature of our model is that it includes two cases (where ATP is produced in excess and otherwise).

For the soliton solutions previously seen to be biologically acceptable, they must be stable. Study of their stability is the purpose of the next section.

IV. STABILITY ANALYSIS

The previous discrete solutions must be stable to be biologically acceptable for the localization and transport of vibrational energy in protein. Here, the stability of these solutions is considered from the view point of both the map orbit stability and the corresponding dynamical stability.

A. Mapping stability

Using the map approach technique [8,34,37–39], and defining $p_n = u_n$ and $q_n = u_{n-1}$, Eq. (16) is transformed into the following two-dimensional real map:

$$\begin{aligned} p_{n+1} &= (2-\Omega)p_n + \eta\frac{p_n}{1+p_n^2} - \eta\frac{p_n^3}{\left(1+p_n^2\right)^2} - q_n \\ q_{n+1} &= p_n. \end{aligned} \tag{18}$$

A linearly unstable map orbit gives rise to a dynamically stable solution [37]. Moreover, to investigate the mapping stability, the study of the stability of the fixed point of the corresponding 2D map is sufficient. Then, the fixed points of Eq. (18), for which $p_n = q_n$, are located at

$$p_0 = 0, \quad p_{1,2} = \pm\sqrt{\frac{-\Omega \pm \sqrt{\Omega\eta}}{\Omega}}. \tag{19}$$

Knowing that $\eta > 0$ with $\eta = 93\widetilde{\eta}$, $p_{1,2}$ exists if only if $\Omega > 0$ and $\eta \geqslant \Omega$. The Jacobian matrix $\check{J}$ of the map Eq. (18) is given by

$$\begin{bmatrix} (2-\Omega) + \eta\frac{1-p_n^2}{\left(1+p_n^2\right)^2} - \eta\frac{p_n^2\left(3-p_n^2\right)}{\left(1+p_n^2\right)^3} & -1 \\ 1 & 0 \end{bmatrix}. \tag{20}$$

The study of the stability of fixed points requires the evaluation (calculation) of the eigenvalues of the Jacobian $\check{J}$ evaluated at these points. This being done, the fixed points will be an unstable saddle point if $|\lambda_1| > 1$ and $|\lambda_2| < 1$ or vice versa. λ_1 and λ_2 being the eigenvalues of $\check{J}$. Particular attention is given to saddle fixed points due to the fact that they can support homoclinic orbits used to generate bright soliton solutions [37]. On the other hand, we recall that the homoclinic orbits are obtained through the intersection of stable and unstable manifolds. In the top left panel of Fig. 3, the areas marked in blue, red, and yellow are those for which p_0, p_1, and p_2 are unstable saddle nodes, respectively. When we employ the technique of residues as defined in Ref. [38], we obtain that the condition of existence of unstaggererd soliton is $\eta \geqslant \Omega$, with $\eta = 93\widetilde{\eta}$. This condition is shown in the top left panel of Fig. 3 by the area bounded by two straight lines of black color. The condition of existence mentioned above is similar to that in the case of the discrete version of the Vinetskii-Kukhtarev equation [34]. This is probably due to the fact that our model has the same tangent map around zero as the discrete Vinetskii-Kukhtarev equation. However, properties related to nonzero fixed points are different from theirs.

Notice that the area of existence in the top left panel of Fig. 3 contains probably two types of spatially localized solutions: breathers and multibreathers [8]. Because the fixed point is saddle, it is not sufficient by itself to guarantee the existence of stable and unstable manifolds that intersect [9]. This is why we must determine the domain for which the stable and unstable manifolds intersect. Figure 4 corroborates the top left panel of Fig. 3 despite some nuances observed when $\Omega \lesssim 0.08$.

Another illustration of the comments that have been carried out is through the top right and bottom left panels of Fig. 3. From these figures, it clearly reflected that the bright soliton

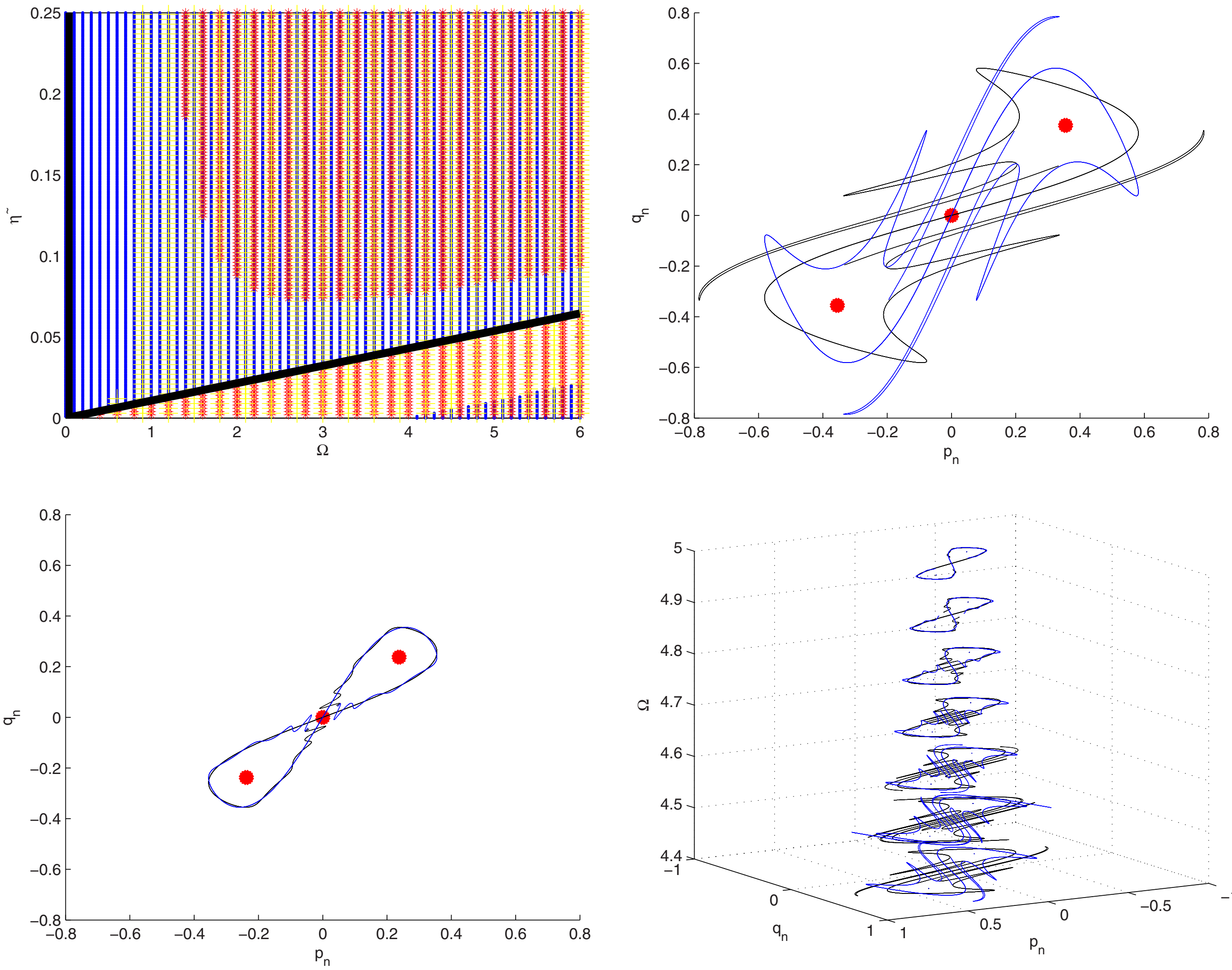

FIG. 3. (Color online) Stability diagram of the fixed points of Eq. (19) (top left panel) in the Ω-$\widetilde{\eta}$ parameter plane. The areas marked in blue, red, and yellow are those for which p_0, p_1, and p_2 are, respectively, unstable saddle nodes. In the top right and bottom left panels, we have intersections of stable and unstable manifolds for $(\Omega,\,\widetilde{\eta}) = (4.4,0.06)$ and $(5,0.06)$, respectively. The red dots being the fixed points. In the bottom right panel, we have the map orbits around the fixed point p_0 according to Ω, $\widetilde{\eta} = 0.06$.

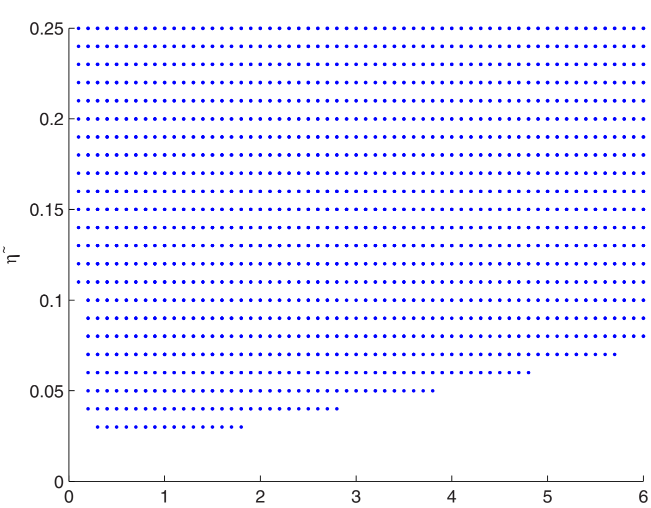

FIG. 4. (Color online) Domain of existence of the intersection of manifolds. Condition of obtaining bright soliton solution.

cannot exist without constraints on the parameters. Moreover, knowing that a much richer tangling structure is equivalent to a richer family of solitons [39], the evolution of map orbits ($\widetilde{\eta} = 0.06$) from $\Omega = 4.4$ to $\Omega = 5$ shows a dimunition of this family of soliton solutions (bottom right panel of Fig. 3). This dimunition continues until $\Omega = 5.58$, where a fold bifurcation occurs. Before that, we have a pitchfork bifurcation that occurs when $\Omega \simeq 4.9$.

At this point, among the previous types (or modes) of solitons discussed, which are most likely to carry in a stable manner the energy of amide-I vibrational excitation through the protein molecules?

B. Linear stability analysis

In this subsection, we will study the stability of DMHS by means of linear stability analysis [40]. Here the DMHS are slightly perturbed:

$$\phi_n = \exp(-i\Omega t)\{u_n + \epsilon[x_n \exp(\lambda t) + y_n \exp(\bar{\lambda} t)]\}, \quad (21)$$

where x_n and y_n are complex, ϵ is a linearization parameter, and λ is the eigenvalue. Add that $\bar{\lambda}$ denotes the complex conjugate of λ, Ω being the frequency seen above. This leads to the linear stability equations:

$$i\lambda\begin{pmatrix}x_n\\ y_n\end{pmatrix}=\begin{bmatrix}-\Omega+\frac{\eta}{1+|u_n|^2}-\frac{3\eta|u_n|^2}{(1+|u_n|^2)^2}+\frac{2\eta|u_n|^4}{(1+|u_n|^2)^3}-\Delta_2 & -\frac{2\eta u_n^2}{(1+|u_n|^2)^2}+\frac{2\eta|u_n|^2u_n^2}{(1+|u_n|^2)^3}\\ \frac{2\eta u_n^2}{(1+|u_n|^2)^2}-\frac{2\eta|u_n|^2u_n^2}{(1+|u_n|^2)^3} & \Omega-\frac{\eta}{1+|u_n|^2}+\frac{3\eta|u_n|^2}{(1+|u_n|^2)^2}-\frac{2\eta|u_n|^4}{(1+|u_n|^2)^3}+\Delta_2\end{bmatrix}\begin{pmatrix}x_n\\ y_n\end{pmatrix}. \qquad (22)$$

Among the $2N$ eigenvalues λ, if at least one has a strictly positive real part, a DMHS is spectrally unstable. Solving numerically Eq. (22), we obtain the eigenvalue spectrum for strongly localized sc and bc modes.

A linear analysis of stability of DMHS composed of soliton belonging to sc mode is carried out by solving numerically the eigenvalue problem (EVP) described by Eq. (22) where u_n is the solution found numerically in the previous section. The results of this analysis are shown in Figs. 5 and 6. Figure 5 is concerning the symmetric two-hump solitons normalized for four values of ℓ_2: 4, 8, 12, and 32. The corresponding eigenvalues spectrum shows that the intensity of the instability decreases as ℓ_2 increases. After checking intermediate values, we note that $\ell_\delta^* \approx 32$ is the threshold value where the solution becomes stable. A similar phenomenon is observed in Fig. 6 for four-hump solitons when $\ell_\delta^* \approx 50$. Thus, the stability of multihump solitons depends on the value of ℓ contrary to what is observed in optics (see Ref. [33]). We further note that the stability of multisoliton depends on ℓ_δ. In fact, ℓ_δ increases as δ increases. As an explanation, we can say that the instability of our multisoliton for values of ℓ_δ below the ℓ_δ^* is probably due to interactions between the δ present solitons. This is why a large number of peaks (δ) leads to great interaction between them, hence a large distance between them to stabilize. This explains the reasons for which we have $\ell_2^* < \ell_3^* < \ell_4^*$.

A numerical evolution of DMHS having at least one soliton with bc mode, by means of fourth-order Runge-Kutta scheme with a suitable choice of time step and absolute tolerance (10^{-10}) in order to ensure the conservation of energy and normalization condition, is performed. It appears that this type of solutions is unstable as we shown in Fig. 7. Indeed, the bc solition of DMHS turns on sc soliton during the evolution of DMHS. A similar fact was noted in Ref. [41], where only onsite single-hump solitons are stable.

C. Existence and stability diagrams of sc DMHS solutions

We proceed to exploring the existence and stability diagrams for all observed types of sc DMHS in the parameter space $(\Omega,\widetilde{\eta})$. It appears from Fig. 8 (top left and bottom right panels) that the regions where DMHS exist decrease as the number of humps increase. For the case of four-hump solitons it is reduced to a very thin region of parameter space. Insets of these figures illustrate the case where the local compression prevails over the local dilatation ($\widetilde{\eta} > 1$). Stability of two-hump soliton with $\ell_2 = 32$ is displayed in the bottom left panel of Fig. 8. It emerges that the increase of interpeak separation ℓ_2 does not make all of the solution stable in the parameter space. It being understood that for $\ell_2 < 32$, almost all two-hump solitons are unstable. Similar to two-hump solitons, almost all four-hump solitons are unstable for $\ell_4 < 50$ and stable for $\ell_4 = 50$ (see the bottom right panel of Fig. 8). This fact reaffirms that interpeak separation has a stabilizing effect on the solutions. The bottom left panel of Fig. 8 underpins this observation. Otherwise, since the magnitude of instability decreases as the interpeak separation

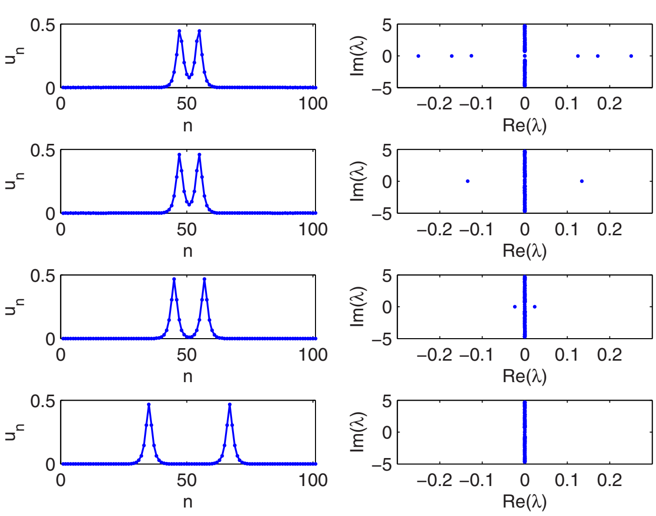

FIG. 5. (Color online) Profiles of two−hump solitons (left column) and their correponding eigenvalue spectrum (right column) with increasing (from top to bottom) values of ℓ_2: $\ell_2 = 4$; 8; 12 and 32. $\Omega \approx 3.6$, $\widetilde{\eta} \approx 0.0464$.

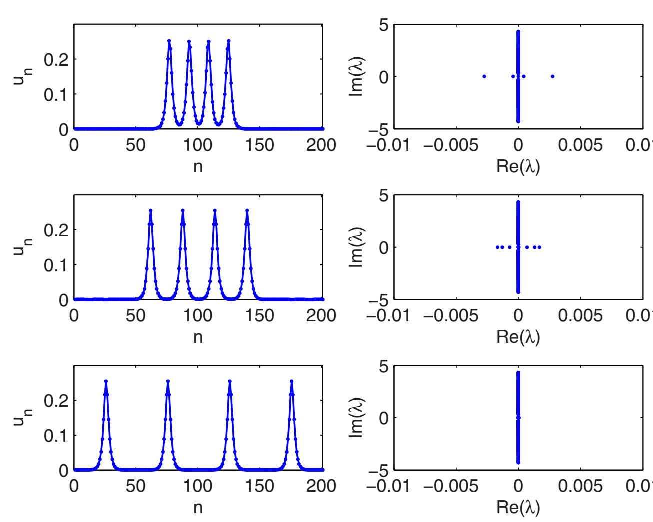

FIG. 6. (Color online) Profiles of four−hump solitons (left column) and their correponding eigenvalue spectrum (right column) with increasing (from top to bottom) values of ℓ_4: ℓ_4 =16; 26 and 50. $\Omega \approx 4.9$, $\widetilde{\eta} \approx 0.056$.

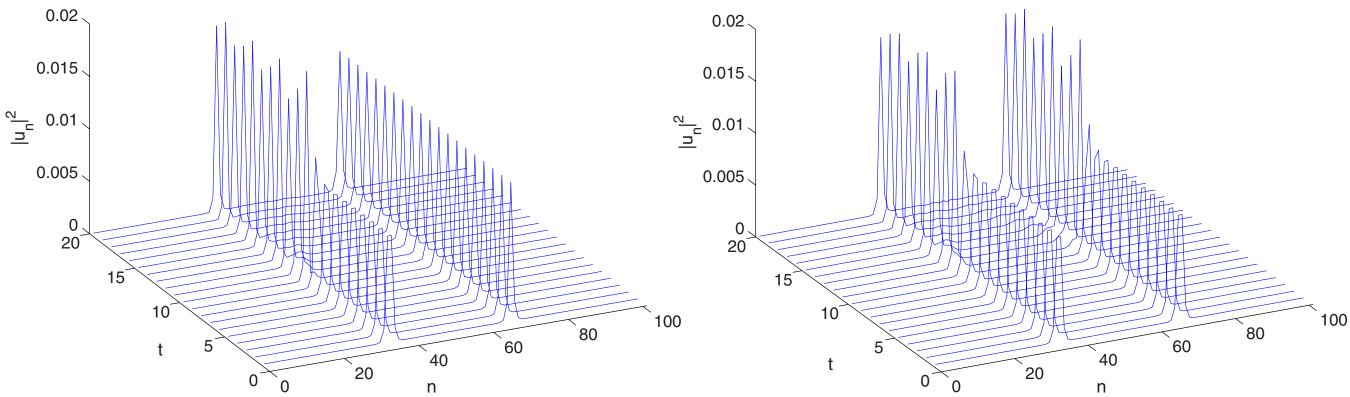

FIG. 7. (Color online) Development of instability of two-hump solitons having at least one intersite soliton for $[(\Omega,\widetilde{\eta}) = (100.9,1.1)]$. The left and right panels correspond to bc-sc mode and bc-bc mode, respectively.

increases [42], the strength of higher-order nonlinearity in our saturable DNLS may enhance the stability. Indeed, it is well known that the magnitude of instability decreases by increasing the strength of nonlinearity of Cubic DNLS [42].

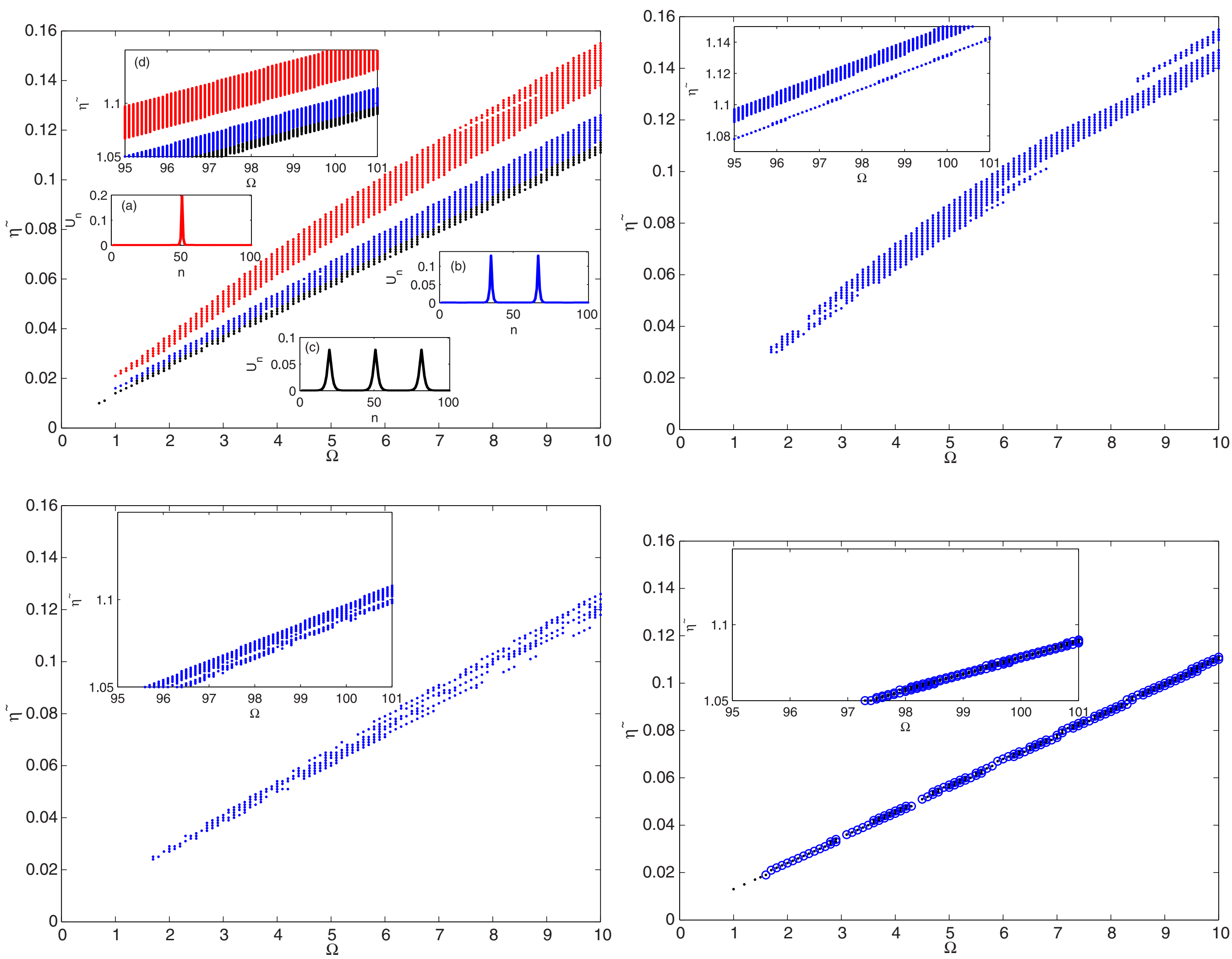

FIG. 8. (Color online) Existence and stability diagrams for all observed types of sc DMHS solutions. In the top left panel, we have the existence diagram for one-hump solitons (red), two-hump solitons (blue), and three-hump solitons (black). Inset (d) shows the case where $\widetilde{\eta} > 1$. Other insets, (a), (b), and (c), are related to observed types of sc DMHS. The stability diagram of one-hump and two-hump ($\ell_2 = 32$) solitons is shows in the top right and bottom left panels, respectively. The bottom right figure illustrates the existence (dot) and stability (circle) diagram for four-hump ($\ell_4 = 50$) solitons. Insets show the case where $\widetilde{\eta} > 1$.

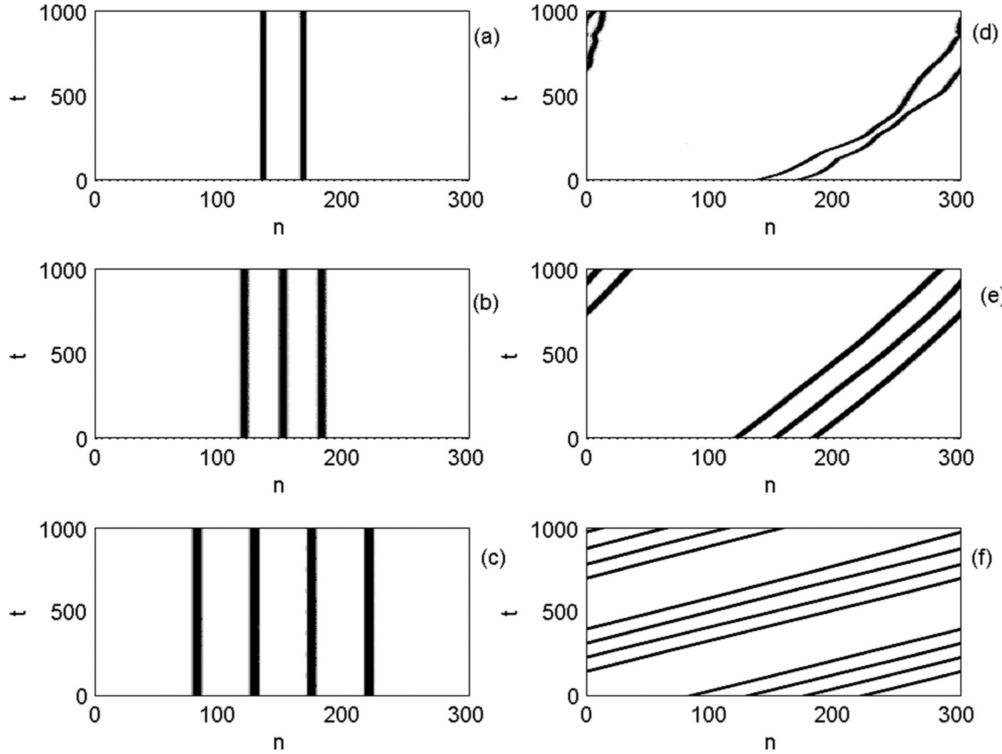

FIG. 9. Density plot $|\phi_n|^2$ for not kicked (a) two-hump, (b) three-hump, (c) four-hump solitons and their kicked counterparts, (d), (e), and (f), respectively. We have (d) $\varpi = 0.55$, $\Omega \approx 3.6$, $\widetilde{\eta} \approx 0.0464$; (e) $\varpi = 0.3$, $\Omega \approx 5.635$, $\widetilde{\eta} \approx 0.065$; (f) $\varpi = 0.3$, $\Omega \approx 4.9$, $\widetilde{\eta} \approx 0.056$; respectively. Mobility is achieved for $\Omega \simeq \eta(\frac{1}{1+\alpha^2})$, (d) $\alpha = 0.4777$, (e) $\alpha = 0.2765$, (f) $\alpha = 0.2549$.

Here the enhancement of the stability is justified by the fact that the strength of higher-order saturable nonlinearity increases the nonlinearity of cubic DNLS equation obtained by expanding in Taylor series the saturable nonlinearities.

At the end of this section, as the evolution of the localized solectron states has suggested their potential as new carriers for fast electric charge transport [28], it emerges that when multipeaked localized solutions are stable, they may be a candidate for energy transport in the protein.

V. MOBILITY OF DISCRETE MULTIHUMP SOLITONS

In this section, we study the DMHS mobility. Note at the outset that the study of bright mobile solution in the DNLS with photorefractive nonlinearity has already been done [23,37,43]. However, for DNLS equation with saturable nonlinearities, mobility of multibreathers has not been yet found. We use here the energy techniques which consist "to push" the localized solution to move through the lattice by means of a variation of the solution initial phase. This is done through the following perturbation:

$$\phi_n(0) = u_n \exp(i\varpi n), \tag{23}$$

where u_n is a stationary solution seen above, and ϖ represents the relative strength.

By applying the kick to two-hump [Fig. 9(a)], three-hump [Fig. 9(b)], and four-hump solitons [Fig. 9(c)], we obtain Figs. 9(d), 9(e), and 9(f), respectively. In these figures, it appears that the mobility is achieved for three-hump solitons, four-hump solitons, and to a more limited extent, two-hump solitons. This is not the case for one-hump solitons. Moreover, in our model, the mobility is achieved for $\Omega \simeq \eta_1[1 + \frac{\eta_2\alpha^2}{\eta_1(1+\alpha^2)}]$, where α is the amplitude of our solutions and $\eta_2 = -\eta_1$. This new condition of mobility depends on the higher-order saturable nonlinearity. For the general case (model where η_1 and η_2 are arbitrary nonlinear coefficients), if $\eta_2 = 0$, this latter condition reduces to $\Omega \simeq \eta$, which is the condition of mobility for the single soliton in the DNLS equation with saturable nonlinearity (see Ref. [37]). In view of the existence diagram, it follows that the sc DMHS are more able to be mobile. In other words, the sc DMHS are more able (with the kick) to overcome the Peierls-Nabarro barrier (PNB).

The main conclusion to be drawn from these observations is that a discrete multihump soliton-like mechanism for vibrational energy transport along the protein chain is possible.

VI. CONCLUSION

In this paper we have shown that the DNLS equation with saturable nonlinearities models the localization and transport of vibrational energy in protein, when a nonlinear and strong exciton-phonon interaction is taken into account. Thus, the model includes conditions of excess ATP and the opposite case. In the absence of the higher-order saturable nonlinearity, the equation model is reduced to the DNLS equation with photorefractive nonlinearity widely used in optics. The multihump (two-hump, three-hump, and four-hump) solitons having sc mode and/or bc mode were sought as solutions of the system and their stability was examined. The linear stability analysis that followed the stability diagram established reveals that the stability of multihump solitons depends not only on the value of the interpeak separation but also on the number of peaks of the solution. The results concerning the existence and stability of the sc DMHS solutions are consolidated in parameter space. A numerical evolution of DMHS having at least one intersite soliton reveals their instability. Finally, the study of the mobility of our solutions has led us to the main conclusion that, depending on the higher-order saturable nonlinearity, a multihump soliton-like mechanism for vibrational energy transport along the protein chain is possible. It will be interesting to study in future works the behavior of two stable discrete multihump solitons during and after collisions.

[1] A. S. Davydov, J. Theor. Biol. **38**, 559 (1973).
[2] P. Xiao-feng, Prog. Biophys. Mol. Bio. **108**, 1 (2012).
[3] G. Careri, U. Buontempo, F. Galluzzi, A. C. Scott, E. Gratton, and E. Shyamsunder, Phys. Rev. B **30**, 4689 (1984).
[4] A. C. Scott, Phys. Rep. **217**, 1 (1992).
[5] S. Flach and C. R. Willis, Phys. Rep. **295**, 181 (1998).
[6] S. Flach and A. V. Gorbach, Phys. Rep. **467**, 1 (2008).
[7] T. Ahn, Nonlinearity **11**, 965 (1998).
[8] T. Bountis, H. W. Capel, M. Kollmann, J. C. Ross, J. M. Bergamin, and J. P. van der Weele, Phys. Lett. A **268**, 50 (2000).
[9] P. G. Kevrekidis, *Discrete Nonlinear Schrödinger Equation: Mathematical Analysis, Numerical Computations and Physical Perspectives*, Springer Tracts Modern Phys., Vol. 232 (Springer, Berlin, 2009).
[10] V. Koukouloyannis, P. G. Kevrekidis, J. Cuevas, and V. Rothos, Physica D **242**, 16 (2013).
[11] A. B. Togueu Motcheyo, C. Tchawoua, M. Siewe Siewe, and J. D. Tchinang Tchameu, Phys. Lett. A **375**, 1104 (2011).
[12] F. Palmero, L. Q. English, J. Cuevas, R. Carretero-Gonzàlez, and P. G. Kevrekidis, Phys. Rev. E **84**, 026605 (2011).
[13] M. Mitchell, M. Segev, and D. N. Christodoulides, Phys. Rev. Lett. **80**, 4657 (1998).
[14] P. G. Kevrekidis, K. Ø. Rasmussen, and A. R. Bishop, Int. J. Mod. Phys. B **15**, 2833 (2001).
[15] V. Koukouloyannis and S. Ichtiaroglou, Phys. Rev. E **66**, 066602 (2002).
[16] V. M. Burlakov, S. A. Kiselev, and V. N. Pyrkov, Phys. Rev. B **42**, 4921 (1990).
[17] K. W. Sandusky, J. B. Page, and K. E. Schmidt, Phys. Rev. B **46**, 6161 (1992).
[18] M. Öster, M. Johansson, and A. Eriksson, Phys. Rev. E **67**, 056606 (2003).
[19] T. R. O. Melvin, A. R. Champneys, P. G. Kevrekidis, and J. Cuevas, Phys. Rev. Lett. **97**, 124101 (2006).
[20] J. Cuevas and J. C. Eilbeck, Phys. Lett. A **358**, 15 (2006).
[21] R. A. Vicencio and M. Johansson, Phys. Rev. E **73**, 046602 (2006).
[22] H. Susanto, P. G. Kevrekidis, R. Carretero-Gonzàlez, B. A. Malomed, and D. J. Frantzeskakis, Phys. Rev. Lett. **99**, 214103 (2007).
[23] T. R. O. Melvin, A. R. Champneys, P. G. Kevrekidis, and J. Cuevas, Physica D **237**, 551 (2008).
[24] C. Mejía-Cortés, R. A. Vicencio, and B. A. Malomed, Phys. Rev. E **88**, 052901 (2013).
[25] A. S. Davydov, J. Theor. Biol. **66**, 379 (1977).
[26] A. S. Davydov, *Theory of Molecular Excitons* (Plenum Press, New York, 1971).
[27] M. Aguero, R. García-Salcedo, J. Socorro, and E. Villagran, Int. J. Theor. Phys. **48**, 670 (2009).
[28] O. G. Cantu Ros, L. Cruzeiro, M. G. Velarde, and W. Ebeling, Eur. Phys. J. B **80**, 545 (2011).
[29] K. Kundu, Phys. Rev. E **61**, 5839 (2000).
[30] L. MacNeil and A. C. Scott, Phys. Scr. **29**, 284 (1984).
[31] E. A. Bartnik, J. A. Tuszynski, and D. Sept, Phys. Lett. A **204**, 263 (1995).
[32] L. A. Cisneros-Ake and A. A. Minzoni, Phys. Rev. E **85**, 021925 (2012).
[33] E. A. Ostrovskaya, Yu. S. Kivshar, D. V. Skryabin, and W. J. Firth, Phys. Rev. Lett. **83**, 296 (1999).
[34] Lj. Hadžievski, A. Maluckov, M. Stepić, and D. Kip, Phys. Rev. Lett. **93**, 033901 (2004).
[35] E. A. Ostrovskaya, S. F. Mingaleev, Yu. S. Kivshar, Y. B. Gaididei, and P. L. Christiansen, Phys. Lett. A **282**, 157 (2001).
[36] F. Mitchell, *Essential Biochemistry for Medicine*, October ed. (John Wiley and Sons, New York, 2010).
[37] A. Maluckov, Lj. Hadžievski, and M. Stepić, Physica D **216**, 95 (2006).
[38] D. Hennig, K. Ø. Rasmussen, H. Gabriel, and A. Bülow, Phys. Rev. E **54**, 5788 (1996).
[39] R. Carretero-Gonzàlez, J. D. Talley, C. Chong, and B. A. Malomed, Physica D **216**, 77 (2006).
[40] A. Maluckov, Lj. Hadžievski, and B. A. Malomed, Phys. Rev. E **76**, 046605 (2007).
[41] M. Stepić, A. Maluckov, M. Stojanović, F. Chen, and D. Kip, Phys. Rev. A **78**, 043819 (2008).
[42] G. Kalosakas, Physica D **216**, 44 (2006).
[43] O. Cohen, R. Uzdin, T. Carmon, J. W. Fleischer, M. Segev, and S. Odoulov, Phys. Rev. Lett. **89**, 133901 (2002).